Resonant Transmission of Electromagnetic Waves in Multilayer Dense-Plasma Structures

Natalia Sternberg and Andrei I. Smolyakov

***Abstract*—An analysis of electromagnetic-wave propagation in dense plasmas when the wave frequency is below the cutoff frequency is presented. Under such conditions, the wave amplitude is usually exponentially attenuated due to collisionless skin effect. It is shown that combining multiple plasma layers of various densities induces a surface-wave resonance, which greatly enhances electromagnetic-wave transmission. Absolute transmission can be achieved even for plasma thickness of many skin depths. Resonant conditions are investigated analytically and numerically.**

***Index Terms*—Electromagnetic-wave transmission, evanescent wave, skin effect, surface-wave resonance.**

I. Introduction

In RECENT years, properties of surface waves have attracted great interest. It has been suggested for some time that surface-wave resonance is responsible for the dramatic enhancement (10^{14}–10^{15} fold) of the radiation from molecules absorbed by a metal surface [1], [2]. It has recently been realized, both in theoretical and experimental studies, that evanescent waves amplified by resonance with a surface wave can be used to transmit a visible range of electromagnetic radiation through metal films [2]. This general ability to guide and manipulate evanescent waves in a media with negative permittivity and negative permeability (metamaterials) became a subject of an extremely vibrant research field with numerous applications in near-field optics, nanophotonics, all optical computer components, etc. [3]–[5].

In this paper, we study resonant propagation of electromagnetic radiation through a specific configuration of dense plasmas. Our goal is to investigate the process of electromagnetic-wave propagation through a layer of dense plasma (with dielectric constant $\varepsilon < 0$) adjacent to layer(s) of less dense plasma ($\varepsilon > 0$). A configuration of layers with dielectric constants of opposite signs can be created artificially in composite structures with alternating layers of metal films and semiconductors in which the electron density can be controlled externally by an electric field. In addition, an external magnetic field can be used to control the plasma dielectric permittivity. A somewhat similar configuration of several layers of dense and rarefied plasmas can arise in laboratory and space plasmas.

Manuscript received February 26, 2009. Current version published July 9, 2009. This work was supported in part by AFOSR Award #FA9550-07-1-0415 and in part by NSERC Canada.

N. Sternberg is with the Department of Mathematics and Computer Science, Clark University, Worcester, MA 01610 USA (e-mail: nsternberg@clarku.edu).

A. I. Smolyakov is with the Department of Physics and Engineering Physics, University of Saskatchewan, Saskatoon, SK S7N 5E2, Canada (e-mail: andrei.smolyakov@usask.ca).

Digital Object Identifier 10.1109/TPS.2009.2020399

It is well known that in any bounded plasma, a thin sheath forms between the quasi-neutral plasma and the material wall. In the quasi-neutral plasma, the ion and electron densities are practically equal, while in the sheath, the electron density is very small [6], [7]. A sheath layer of low electron density also forms at the plasma–vacuum interface if the plasma is immersed into vacuum. As a result, a dense-plasma layer is sandwiched between two layers of low-density plasma. Such three-layer configurations occur near the edge of plasma confinement devices as well as around space vehicles. A typical sheath–plasma–sheath structure was shown to form around an aircraft during hypersonic flight [8]. It is therefore of interest to investigate the resonant electromagnetic-wave propagation through such structures and possible applications to the problem of communication interruption with an aircraft surrounded by dense plasma (the black-out problem) [9]–[13].

General conditions for resonant signal transmission via a two-layer structure were studied in [14] and [15], and a general three-layer structure was considered in [16]. In this paper, we investigate, in detail, the transmission through two- and three-layer structures for a typical plasma that occurs during a hypersonic flight. We use the impedance method, which is compact, can be conveniently applied to multiple plasma layers, and can therefore be used effectively for numerical simulation of smooth profiles. Our results show that the deficiencies of the two-layer model can be mitigated by choosing a symmetric three-layer structure, where the dense plasma is bounded by a layer of rarefied plasma on each side. Indeed, in contrast to a two-layer structure, resonant signal transmission for our three-layer model can be achieved by choosing the width of each boundary layer comparable in size with the width of the dense plasma. Furthermore, the bandwidth of the transmitted wave is much larger than that in the two-layer structure.

This paper is organized as follows. In Section II, we formulate the problem and present the basic equation. In Section III, we discuss the relationship between the wave impedance and the reflection coefficient in a single-layer structure. In Section IV, we discuss the impedance model for multilayer structures and apply it to a two-layer medium. In Section V, we study a symmetric three-layer structure. In Section VI, we discuss the result.

II. Formulation of the Problem and Basic Equations

We consider the propagation of electromagnetic radiation through a multilayer structure as shown in Fig. 1. An electromagnetic wave is incident from a semi-infinite vacuum (air)

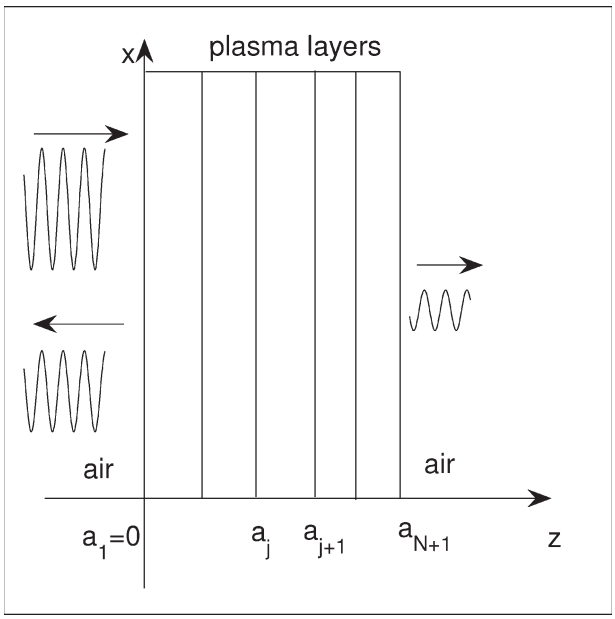

Fig. 1. Schematic representation of electromagnetic-wave propagation through a multilayer medium.

region on the left. The transmitted wave propagates into a semi-infinite vacuum (air) region on the right. In general, there are incident and reflected waves on the left, but there is no reflected wave on the right. When a dense-plasma layer is present within the structure, the reflection coefficient is large, and most of the radiation is reflected due to the skin-effect screening. The question is whether it is possible to create conditions when the reflection is low and most of the radiation is transmitted through the structure.

For simplicity, we consider a 1-D model so that the plasma density varies only in the z-direction. In general, the incident wave has a finite component of the wave vector parallel to the interface (y-direction). We consider a p-polarized wave so that the electromagnetic field is represented by

$$\begin{aligned}\mathbf{E} &= (0, E_y(z), E_z(z)) \exp(iky - i\omega t)\\ \mathbf{H} &= (H_x(z), 0, 0) \exp(iky - i\omega t)\end{aligned} \tag{1}$$

where $k = \sin(\theta)\omega/c$, with c being the speed of light and θ being the angle of incidence. We assume a cold collisionless nonmagnetized plasma with immobile ions in an RF field, such that $\mu = 1$. The plasma dielectric constant is then

$$\varepsilon(z) = 1 - \frac{\omega_{\rm pe}^2(z)}{\omega^2} \tag{2}$$

where

$$\omega_{\rm pe}(z) = \left(\frac{e^2 n(z)}{\varepsilon_0 m}\right)^{1/2}. \tag{3}$$

From the Maxwell equations, one finds the following wave equation for an inhomogeneous plasma

$$\varepsilon \frac{d}{dz}\left(\frac{1}{\varepsilon}\frac{dH_x}{dz}\right) - \gamma^2(\varepsilon, \theta) H_x = 0 \tag{4}$$

where

$$\gamma^2(\varepsilon, \theta) \equiv k^2(\theta) - \varepsilon \frac{\omega^2}{c^2}. \tag{5}$$

In the vacuum region ($\varepsilon = 1$), γ is imaginary and the wave is propagating. In the dense-plasma region with $\omega^2 < \omega_{\rm pe}^2$, γ is real, the wave becomes evanescent, and the amplitude of the transmitted wave is exponentially small. It is, however, possible to amplify the amplitude of the transmitted wave through resonance with the surface-wave eigenmode (see Section III).

For the multilayer structure under consideration, we assume that inside each layer, the plasma density is constant, and thus, γ is constant. Equation (4) can therefore be solved analytically in each layer, where the fundamental solutions are represented by exponential functions. The solutions in neighboring layers are then matched at the interfaces. The matching condition is obtained by integrating (4) over a small interval $[a_j - \delta, a_j + \delta]$, $\delta > 0$, across the interface $z = a_j$. In the limit $\delta \to 0$, this yields continuity of $(dH_x/dz)/\varepsilon$ across the interface. Similarly, one finds from the Maxwell equations that the components H_x and E_y are also continuous.

For a multilayer structure, the transmission problem for (4) can be formulated by the method of transfer functions, where each interface and each uniform region is represented by a 2×2 matrix. This method leads to a cumbersome and computationally intensive final result, which is represented in the form of a product of all of these matrices and their inverses. Instead, we will use an alternative method based on the wave impedance.

III. Impedance and Reflection of a Single-Layer Structure

The relationship between the impedance and the reflection coefficient for a propagating wave in a single layer is well known. We now discuss that relationship for evanescent waves to clarify the exposition and the notation in the following sections.

Consider an electromagnetic wave in a single layer of a uniform density. Consider the representation (1) for the electromagnetic wave field. For a wave propagating to the right (incident wave), $\gamma = ik_z$, $k_z > 0$, and

$$\begin{aligned}H_x(z) &= H_0 \exp(ik_z z)\\ E_y(z) &= E_{y0} \exp(ik_z z)\\ E_z(z) &= E_{z0} \exp(ik_z z).\end{aligned} \tag{6}$$

For a wave propagating to the left (reflective wave), ik_z is replaced by $-ik_z$ in (6). For an evanescent wave decaying in the positive z-direction (we call it an incident wave)

$$\begin{aligned}H_x(z) &= H_0 \exp(-\gamma z)\\ E_y(z) &= E_{y0} \exp(-\gamma z)\\ E_z(z) &= E_{z0} \exp(-\gamma z)\end{aligned} \tag{7}$$

for $\gamma > 0$, while for an evanescent wave growing in the positive z-direction (we call it a reflected wave), $-\gamma$ is replaced by

γ in (7). Here, H_0, E_{y0}, and E_{z0} are the amplitudes of the corresponding wave fields.

The local wave impedance is defined as

$$Z = -\frac{E_y}{H_x} = -\frac{i}{\omega\varepsilon_0\varepsilon H_x}\frac{dH_x}{dz}. \tag{8}$$

For an incident propagating wave, the impedance is therefore given by

$$Z = \frac{k_z}{\omega\epsilon_0\epsilon}. \tag{9}$$

In particular, in a vacuum layer ($\epsilon = 1$), the impedance of a propagating electromagnetic wave is

$$Z_0 = \frac{k_v}{\omega\epsilon_0} \tag{10}$$

where $k_v = \cos(\theta)\omega/c$. The impedance of an incident evanescent wave can also be defined by (8), which yields

$$Z = \frac{i\gamma}{\omega\epsilon_0\epsilon}. \tag{11}$$

Note that for both the propagating and evanescent cases, the impedance of the corresponding reflective waves has the opposite sign. Furthermore, in a uniform medium, ϵ is constant, and the impedance of a single wave is constant throughout the layer.

Suppose that the uniform layer under consideration is of width l and dielectric permittivity ϵ. Solving (4) inside the layer, we find that the magnetic wave field can be represented in the form

$$H_x(z) = H_0\left(\exp(-\gamma z) + \Gamma\exp(\gamma z)\right) \tag{12}$$

for $0 < z < l$, where Γ is the reflection coefficient. The electric field distribution within the layer is then

$$E_y = \frac{i\gamma}{\omega\epsilon_0\epsilon}H_0\left(-\exp(-\gamma z) + \Gamma\exp(\gamma z)\right) \tag{13}$$

and we define the local impedance by

$$Z(z) = -\frac{E_y(z)}{H_x(z)}. \tag{14}$$

For the electromagnetic wave field given by (12) and (13), the local impedance becomes

$$Z(z) = Z_{\rm ch}\frac{\exp(-\gamma z) - \Gamma\exp(\gamma z)}{\exp(-\gamma z) + \Gamma\exp(\gamma z)} \tag{15}$$

where

$$Z_{\rm ch} = \frac{i\gamma}{\omega\epsilon_0\epsilon} \tag{16}$$

is the characteristic impedance of the medium, which is exactly the impedance of the incident wave [see (11)]. Note that unlike in the case of a single wave, the local impedance given by (15) is not constant throughout the layer.

Let $Z_{\rm in} = Z(0)$ be the input impedance, and let $Z_L = Z(l)$ be the load impedance. Then, according to (15)

$$Z_{\rm in} = Z_{\rm ch}\frac{1-\Gamma}{1+\Gamma} \tag{17}$$

$$Z_L = Z_{\rm ch}\frac{\exp(-\gamma l) - \Gamma\exp(\gamma l)}{\exp(-\gamma l) + \Gamma\exp(\gamma l)}. \tag{18}$$

Equations (17) and (18) yield the following relationship between the input impedance and the load impedance:

$$Z_{\rm in} = Z_{\rm ch}\frac{Z_L + Z_{\rm ch}\tanh(\gamma l)}{Z_{\rm ch} + Z_L\tanh(\gamma l)}. \tag{19}$$

Thus, (19) gives the relationship between the impedance $Z(0)$ at the left boundary of the plasma layer and the impedance $Z(l)$ at the right boundary of the plasma layer.

Note that the earlier discussion holds for evanescent waves ($\gamma > 0$) as well as for propagating waves ($\gamma = -ik_z$, $k_z > 0$).

For the semi-infinite vacuum region with $z < 0$, it holds that $Z_{\rm ch} = Z_0$, and we find that

$$\Gamma = \frac{Z_0 - Z_L}{Z_L + Z_0} \tag{20}$$

where $Z_L = Z(0)$.

Note that (19) defines the input impedance of the plasma layer in terms of the impedance of the load and the characteristic impedance of the layer. Equation (20) defines the reflection coefficient for the wave incident from a semi-infinite vacuum region with the characteristic impedance Z_0 onto the impedance load Z_L.

Since the impedance is a continuous function, one can match the corresponding values at each interface and obtain the impedance of the whole structure by applying (19) sequentially. This will be discussed in the following section.

IV. Impedance and Reflection in a Multilayer Structure

The ideas of the previous section can be easily generalized to obtain the formal solution of the transmission problem for a multilayer structure and a general expression for the transmission coefficient.

Suppose that there are N plasma layers altogether shown in Fig. 1. Suppose that l_j is the width of the jth layer. Suppose that the position of each interface is at $z = a_j$ with $a_1 = 0$. To the left and to the right of the plasma layers, for $z < 0$ and $z > a_{N+1}$, there are semi-infinite vacuum (air) regions. Consider an arbitrary single uniform plasma layer in Fig. 1, for example, the jth layer. Then, $a_j < z < a_{j+1}$, the width of the layer is $l_j = a_{j+1} - a_j$, and the dielectric permittivity of the layer is ε_j, which is constant. The magnetic field inside the layer can be represented in the form

$$H_x = H_j\left(\exp(-\gamma_j z) + \Gamma_j\exp(\gamma_j z)\right) \tag{21}$$

where $\gamma_j = \gamma(\varepsilon_j, \theta) > 0$ is given by (5), H_j is the amplitude of the incident wave, and Γ_j is the reflection coefficient. Here and below, the index j refers to the jth layer.

We consider the value of the impedance at $z = a_j$ as the input impedance and denote it by $Z_{\rm in}^j$. The value of the impedance at $z = a_{j+1}$ is the load impedance, and we denote it by Z_L^j. Then, following the procedures in the previous section, we find that the input impedance can be expressed in terms of the load impedance as follows:

$$Z_{\rm in}^j = Z_j \frac{Z_L^j + Z_j \tanh(\gamma_j l_j)}{Z_j + Z_L^j \tanh(\gamma_j l_j)} \tag{22}$$

where

$$Z_j = \frac{i\gamma_j}{\omega \varepsilon_0 \varepsilon_j} \tag{23}$$

is the characteristic impedance of the jth layer. Since the impedance is a continuous function, we can set

$$Z_{\rm in}^{j+1} = Z(a_{j+1}) = Z_L^j \tag{24}$$

and (22) yields the following recursion formula for the computation of the local impedance at each interface $Z(a_j)$:

$$Z(a_j) = Z_j \frac{Z(a_{j+1}) + Z_j L_j}{Z_j + Z(a_{j+1}) L_j} \tag{25}$$

for all $j = 1, \ldots, N$, where

$$L_j = \tanh(\gamma_j l_j). \tag{26}$$

Note that L_j is a function of θ, ϵ_j, and l_j. For $\gamma_j > 0$ and $l_j > 0$, it follows that $0 < L_j < 1$.

In the vacuum region to the right of the multilayer structure, there is only the transmitted electromagnetic wave, and therefore, $Z(a_{N+1}) = Z_0$, where Z_0 is the vacuum impedance. Thus, in order to compute the impedance at each interface $z = a_1 = 0, \ldots, z = a_{N+1}$, we can use the recursion formula (25) starting at $Z(a_{N+1}) = Z_0$.

For the semi-infinite vacuum region $z < 0$ (see Fig. 1), the load impedance is $Z_L = Z(a_1) = Z(0)$, and according to (20), the reflection coefficient is

$$\Gamma = \frac{Z_0 - Z(0)}{Z(0) + Z_0}. \tag{27}$$

Thus, the calculation of the reflection coefficient for a propagating wave when it reaches a multilayer plasma structure can be reduced to the calculation of the impedance at the plasma–vacuum interface. Full transparency of the medium can be achieved when $\Gamma = 0$. In this case, the impedance at $z = 0$ has to be exactly the vacuum impedance.

To simplify the computations, we normalize the impedance to the vacuum impedance

$$\tilde{Z} = \frac{Z}{Z_0}. \tag{28}$$

Observe that $\tilde{Z}$ satisfies the recursion formula (25) with the initial condition $\tilde{Z}(a_{N+1}) = 1$, and the transparency condition becomes

$$\tilde{Z}(0) = 1. \tag{29}$$

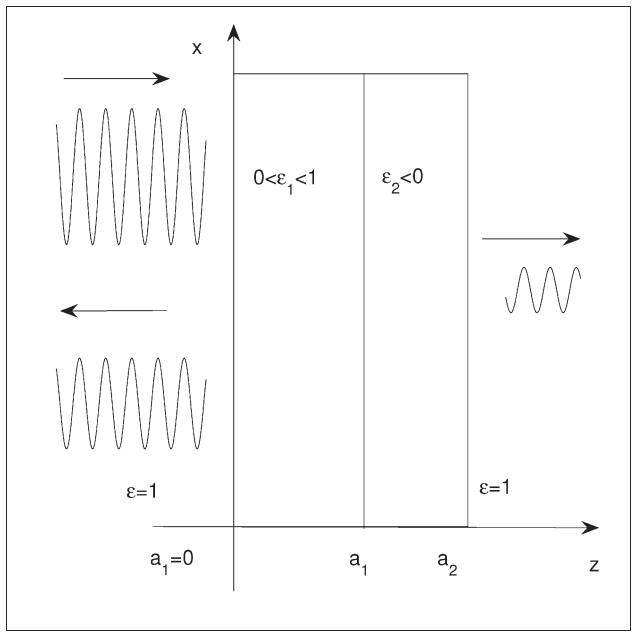

Fig. 2. Schematic representation of electromagnetic-wave propagation through a two-layer medium.

In what follows, we will use Z instead of $\tilde{Z}$, but we will always mean the normalize impedance.

In order to illustrate the resonant excitation of surface modes and resonant transmission, consider a two-layer structure in Fig. 2. Then, $N = 2$, $a_1 = 0$, and $Z(a_3) = 1$. Applying (25) twice, we find that

$$Z(a_2) = Z_2 \frac{1 + Z_2 L_2}{Z_2 + L_2} \tag{30}$$

$$Z(0) = Z_1 \frac{Z(a_2) + Z_1 L_1}{Z_1 + Z(a_2) L_1}. \tag{31}$$

Substituting (30) into (31) and using the transparency conditions (29), we find that the two-layer structure is transparent if

$$-Z_2^2 L_1 L_2 + Z_1^2 L_1 L_2 + Z_1 Z_2^2 L_2 + Z_1^2 Z_2 L_1 - Z_1 L_1 - Z_2 L_1 = 0. \tag{32}$$

Suppose that the second layer is a sufficiently dense plasma, so that the electromagnetic wave through that layer is evanescent, i.e., Z_2 is imaginary and L_2 is real. Then, (32) has a solution if the wave through the first layer (the boundary layer) is also evanescent, i.e., Z_1 is imaginary and L_1 is real. Equation (32) is therefore equivalent to the following system of equations:

$$Z_1^2 = Z_2^2 \tag{33}$$

$$Z_1 Z_2^2 L_2 + Z_1^2 Z_2 L_1 - Z_1 L_2 - Z_2 L_1 = 0 \tag{34}$$

which yield the solution

$$Z_1 = -Z_2 \qquad L_1 = L_2 \tag{35}$$

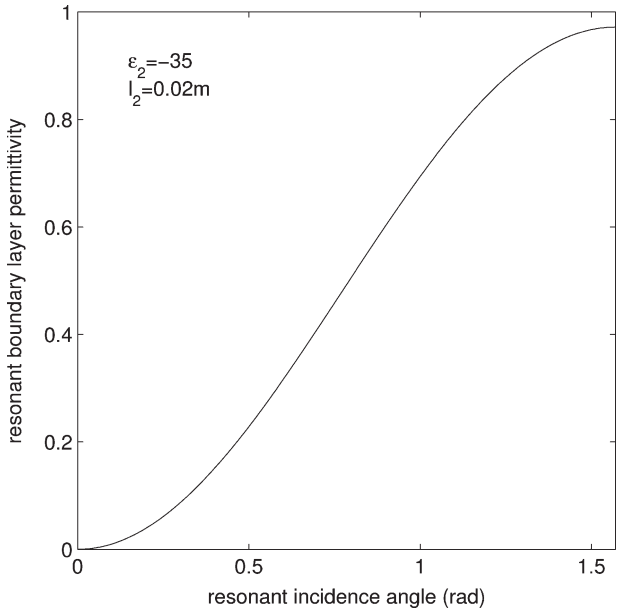

Fig. 3. Resonant boundary layer permittivity versus resonant incidence angle for a two-layer structure.

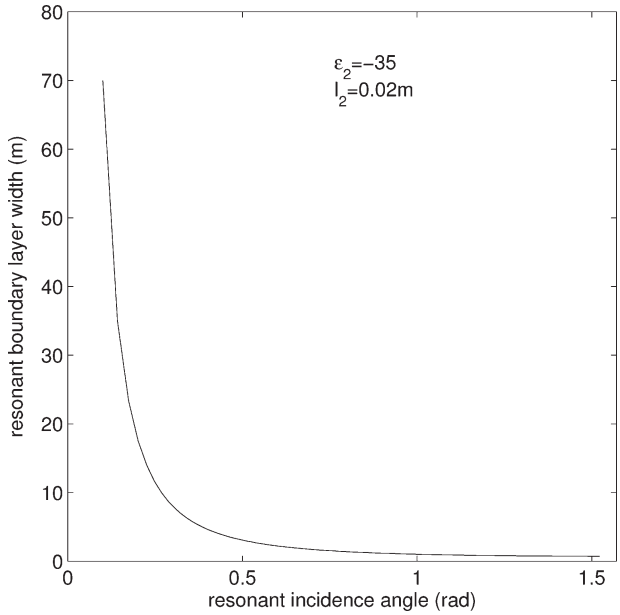

Fig. 4. Resonant boundary layer width versus the incidence angle in a two-layer structure.

or equivalently

$$\frac{\gamma_1}{\epsilon_1} = -\frac{\gamma_2}{\epsilon_2} \tag{36}$$

$$l_1 = \frac{\gamma_2}{\gamma_1} l_2. \tag{37}$$

Furthermore, by using (5) and (36), we find that the absolute transparency occurs if

$$\theta = \arcsin\left(\sqrt{\frac{\epsilon_1 \epsilon_2}{\epsilon_2 + \epsilon_1}}\right). \tag{38}$$

Equation (36) is exactly the dispersion relation of the surface wave between the two layers, which is in resonance with the incident wave. This is the first condition needed for absolute transparency [14], [15]. Note from (36) that for absolute transparency, ϵ_1 and ϵ_2 must have opposite signs. The second condition for absolute transparency is given by (37). It shows the relationship between the widths of the layers and their permittivity, which is the matching condition required for absolute transparency. In particular, for a sufficiently dense plasma, $\gamma_2/\gamma_1 > 1$ holds, and hence, $l_1 > l_2$.

Observe from (38) that $\theta = 0$ cannot be a resonant angle. Furthermore, for a given permittivity ϵ_2, there is a one-to-one correspondence between the resonant incidence angle and the permittivity of the corresponding resonant boundary layer ϵ_1. If, in addition, the plasma width l_2 is given, then there is also a one-to-one correspondence between the resonant incident angle and the resonant width of the boundary layer. This is shown in Figs. 3 and 4 for $\epsilon = -35$ and $l_2 = 0.02$ m. Note that a larger resonant incidence angle requires a larger resonant boundary layer permittivity and a smaller resonant boundary layer width. Still, the boundary layer width is quite large, compared to the width of the plasma layer. For example, the resonant incidence angle $\theta = 1.2910$ requires $\epsilon_1 = 0.9$ and $l_1 = 0.78$ m. Fig. 5 shows the dependence of the magnitude of the reflection coefficient Γ on the incidence angle and illustrates that the incidence angle $\theta = 1.2910$, indeed, produces resonant conditions, i.e., $\Gamma = 0$.

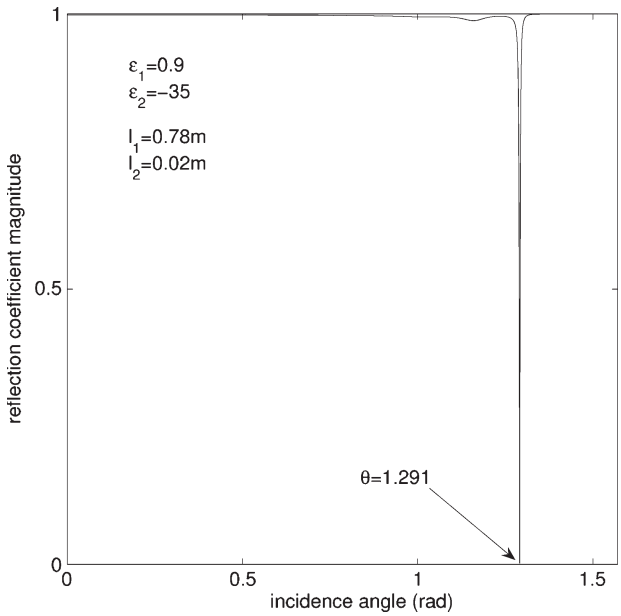

Fig. 5. Magnitude of the reflection coefficient versus the incidence angle for a two-layer medium; the resonant angle is $\theta = 1.2910$.

Note that $\epsilon_2 = -35$ corresponds to the plasma frequency $\omega_{\rm pe}/(2\pi) = 6$ GHz typical around the aircraft during hypersonic flight and the incident frequency $\omega/(2\pi) = 1$ GHz which is within the GPS range [8]. Throughout this paper, we will use this value of ϵ_2 together with the value $l_2 = 0.02$ m for the plasma width.

In summary, the impedance method provides a simple way for obtaining analytical results for resonant electromagnetic-wave transmission in a two-layer structure. In the following

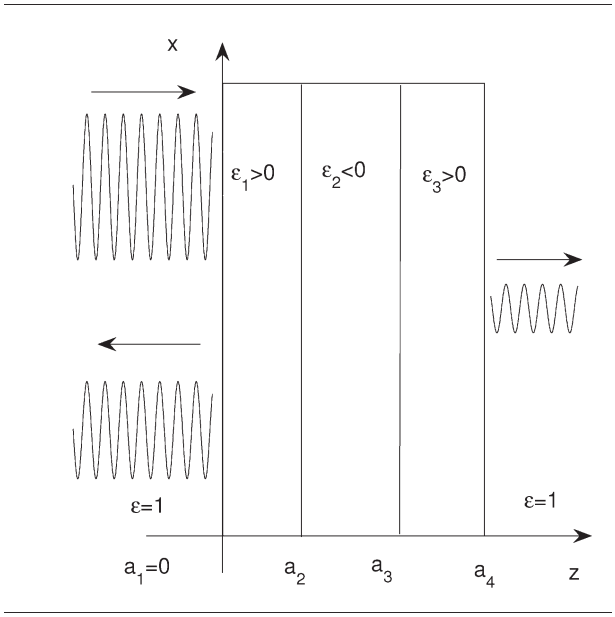

Fig. 6. Schematic representation of electromagnetic-wave propagation through a three-layer medium.

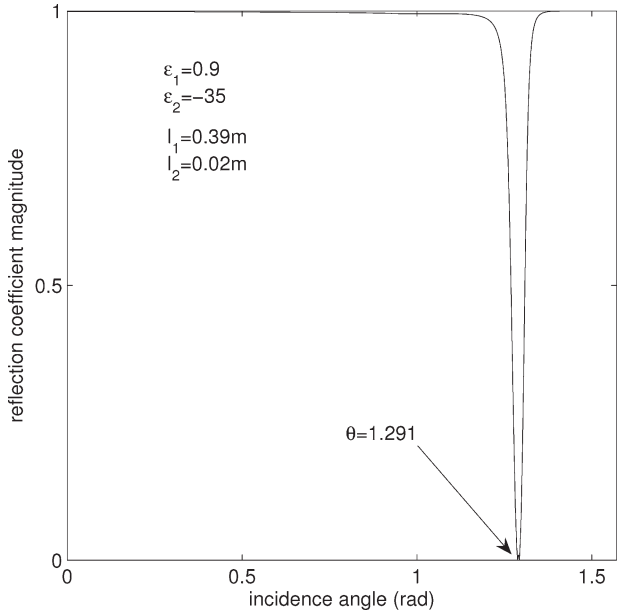

Fig. 7. Magnitude of the reflection coefficient versus incidence angle in a three-layer structure; the resonant incidence angle is $\theta = 1.2910$.

section, we will use the impedance method to study a three-layer structure.

V. Transparency of a Symmetric Three-Layer Structure

Consider a three-layer structure shown in Fig. 6. The dense-plasma layer is nested between two other layers. For simplicity, assume that the two outside layers have the same width and permittivity, i.e., $l_1 = l_3$, $\epsilon_1 = \epsilon_3$, and hence, $L_1 = L_3$ and $Z_1 = Z_3$. By using (25) for the normalized impedance, we find that

$$Z(a_3) = Z_1 \frac{1 + Z_1 L_1}{Z_1 + L_1} \tag{39}$$

$$Z(a_2) = Z_2 \frac{Z(a_3) + Z_2 L_2}{Z_2 + Z(a_3) L_2} \tag{40}$$

$$Z(0) = Z_1 \frac{Z(a_2) + Z_1 L_1}{Z_1 + Z(a_2) L_1} \tag{41}$$

and from the transparency condition (29), we find the following condition for absolute transparency:

$$L_2 L_1^2 \left(Z_1^4 - Z_2^2\right) + 2 L_1 Z_1 Z_2 \left(Z_1^2 - 1\right) + L_2 Z_1^2 \left(Z_2^2 - 1\right) = 0. \tag{42}$$

We can find a solution of (42) by setting

$$Z_1^2 = Z_2^2. \tag{43}$$

Then

$$L_1^2 + \frac{2}{L_2} \frac{Z_1}{Z_2} L_1 + 1 = 0 \tag{44}$$

and therefore

$$L_1 = -\frac{1}{L_2} \frac{Z_1}{Z_2} \pm \sqrt{\frac{1}{L_2^2} - 1}. \tag{45}$$

For a sufficiently dense-plasma layer, Z_2 is imaginary. Assume that Z_1 is also imaginary, i.e., the electromagnetic wave in each layer is evanescent. Then, since $0 < L_1 < 1$, it follows that

$$Z_1 = -Z_2 \tag{46}$$

and since $0 < L_2 < 1$, we find that

$$L_1 = \frac{1}{L_2} - \sqrt{\frac{1}{L_2^2} - 1}. \tag{47}$$

Similarly to the two-layer structure, (43) is the dispersion relation of the surface wave generated by the sharp interface between the layers. As in the two-layer problem, (43) yields the relationship (36), which, in turns, yields (38) for the computation of the resonant incidence angle. Furthermore, as in the two-layer problem, for the surface-wave-induced resonance, (36) yields $0 < \epsilon_1 < \sin^2(\theta) < 1$. Moreover, for a given L_2, since $L_1 = \tanh(\gamma_1 l_1)$, we can find the width of the boundary layers

$$l_1 = \frac{1}{\gamma_1} \tanh^{-1}(L_1). \tag{48}$$

In particular, choosing the same parameters as in the previous section, namely, $\epsilon_1 = 0.9$, $\epsilon_2 = -35$, and $l_2 = 0.02$ m, we find that the resonant angle is $\theta = 1.2910$ and the corresponding boundary layer width is $l_1 = 0.39$ m. This is illustrated in Figs. 7 and 8 which show the dependence of the magnitude of the reflection coefficient Γ on the incidence angle and the boundary layer width for a three-layer structure. Note that as for

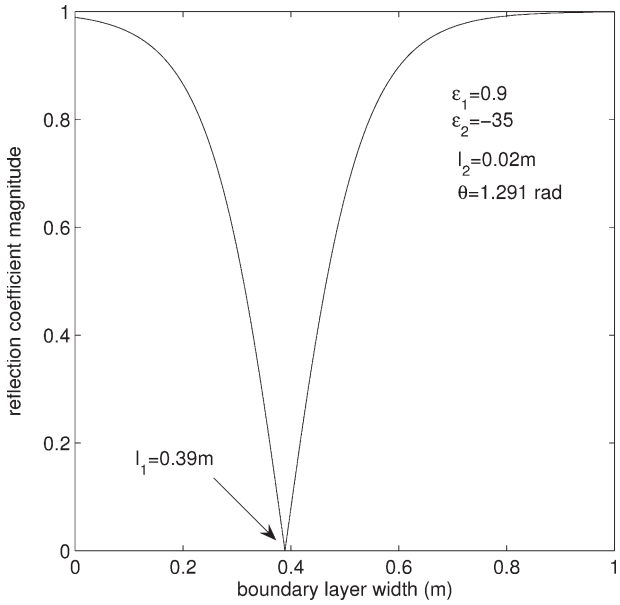

Fig. 8. Magnitude of the reflection coefficient versus boundary layer width in a three-layer structure; the boundary layer width is $l_2 = 0.39$ m.

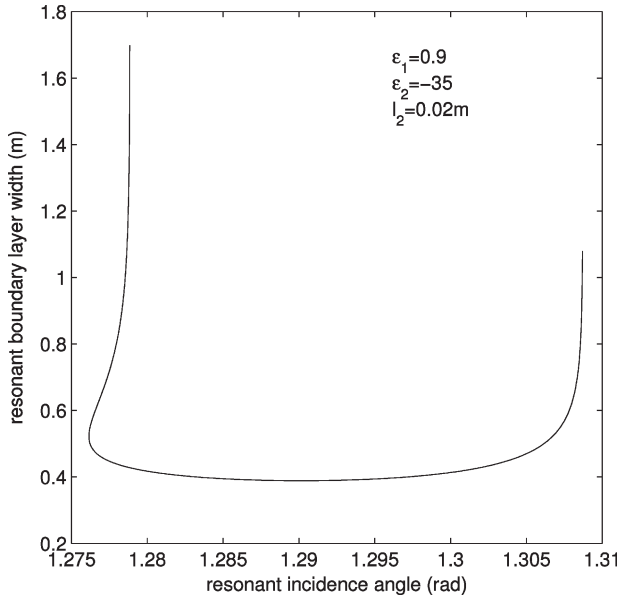

Fig. 9. Boundary layer width versus the incidence angle in a three-layer structure; the incidence angle is in the interval [1.2761554, 1.3087].

a two-layer structure, the resonant incidence angle in a three-layer structure is also $\theta = 1.2910$, but the resonant boundary layer width is half of that in a two-layer structure. Note also that the bandwidth in a three-layer structure is much wider than in a two-layer structure.

A two-layer structure permits only one solution of the transparency condition (32) for $\epsilon_2 < 0$, namely, $Z_1 = -Z_2$. A three-layer structure, however, permits more solutions of the corresponding transparency condition (42). In order to find those solutions, first note that if both Z_1 and Z_2 are imaginary, the quadratic equation (44) has a real solution only if $Z_1 Z_2 > 0$. Therefore, $0 < \epsilon_1 < \sin^2(\theta)$, and we obtain the following bounds for the resonant incidence angle:

$$\arcsin(\sqrt{\epsilon_1}) < \theta < \frac{\pi}{2}. \tag{49}$$

We consider the resonant angle θ as a parameter of the problem while fixing $\epsilon_1 = 0.9$, $\epsilon_2 = -35$, and $l_2 = 0.02$ m. For each θ, we can solve the quadratic equation (44) for L_1 and then find the corresponding resonant boundary layer width l_1 according to (48). Observe that since l_1 is real, we are interested only in solutions L_1 of (42) such that $0 < L_1 < 1$. Our computations show with high accuracy that for $1.2761554 < \theta \leq 1.27885$ and $1.533614 < \theta < \pi/2$, there are two real solutions of (42) which are both positive and less than one. Moreover, for $1.27885 < \theta \leq 1.3087$, there are two real solutions of (42): one greater than one and the other one less than one. Furthermore, there are two positive solutions of multiplicity 2 less than 1: one for $\theta = 1.2761554$ and the other one for $\theta = 1.533614$. The resonant boundary layer widths corresponding to all those solutions are shown in Figs. 9 and 10. In Fig. 9, one can see the unique resonant boundary layer width for $\theta = 1.2761554$. Furthermore, there are two resonant boundary layer widths for each $1.2761554 < \theta \leq 1.27885$, and again a unique resonant boundary layer width for each $1.27885 < \theta \leq 1.3087$. It is

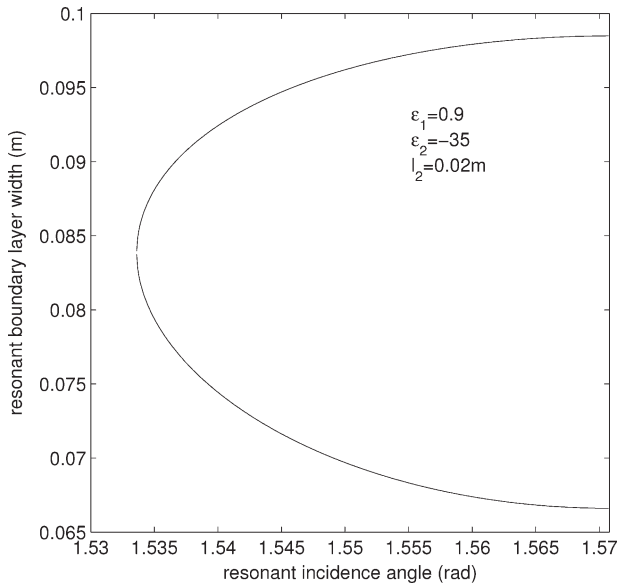

Fig. 10. Boundary layer width versus the incidence angle in a three-layer structure; the incidence angle is in the interval [15.33614, 1.57].

interesting to observe that in Fig. 9, the resonant boundary layer width is minimal for $\theta = 1.2910$, which is exactly the special case of surface-wave resonance considered earlier. In Fig. 10, there is a unique resonant boundary layer width for $\theta = 1.533614$, while for each $\theta > 1.533614$, there are two resonant boundary layer widths. Observe that the boundary widths in Fig. 9 are much larger than the plasma width l_2, while in Fig. 10, particularly on the lower branch, the boundary layer widths and the plasma width are comparable in size.

Recall that Fig. 8 shows the behavior of the magnitude of the reflection coefficient Γ as a function of the resonant boundary layer width for $\theta = 1.2910$. This behavior is representative for all incidence angles within the interval (1.27885, 1.3087]. For

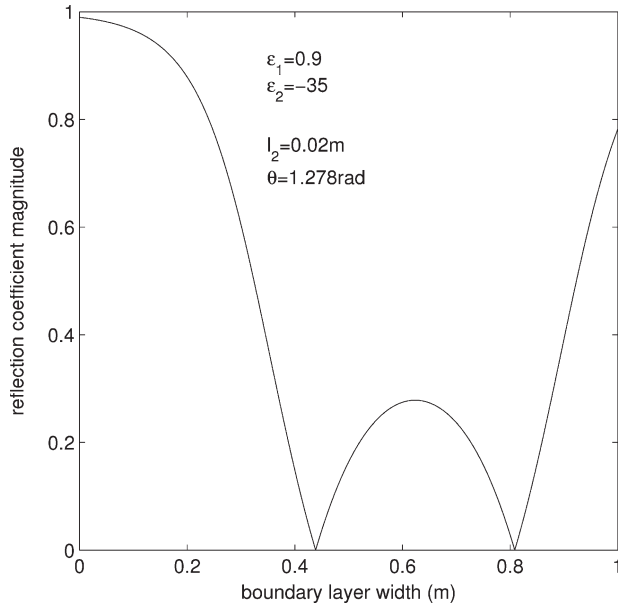

Fig. 11. Magnitude of the reflection coefficient versus width of the boundary layer in a three-layer structure for the resonant incidence angle $\theta = 1.278$; the two corresponding resonant widths are 0.44 and 0.81 m.

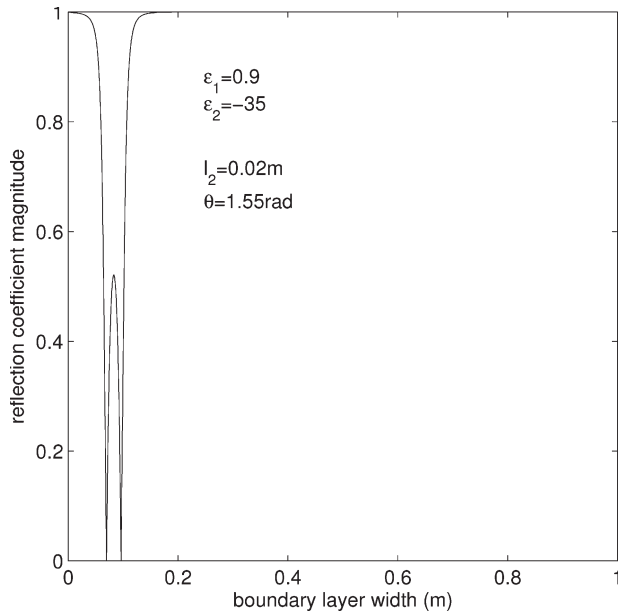

Fig. 12. Magnitude of the reflection coefficient versus width of the boundary layer in a three-layer structure for the resonant incidence angle $\theta = 1.55$; the two corresponding resonant widths are 0.07 and 0.096 m.

each of those angles, there is a unique resonant boundary layer width, and that width is quite large compared to l_2. Figs. 11 and 12 show examples of the behavior of the magnitude of the reflection coefficient as a function of the resonant boundary layer width for θ in the corresponding interval discussed earlier. In Fig. 11, we chose $\theta = 1.278$ as a representative of the interval (1.2761554, 1.27885]. As expected, there are two resonant boundary layer widths for that angle, and those widths are much larger than the plasma width l_2. Fig. 12 shows the behavior of the reflection coefficient as a function of the resonant boundary layer width for $\theta = 1.55$, which represents

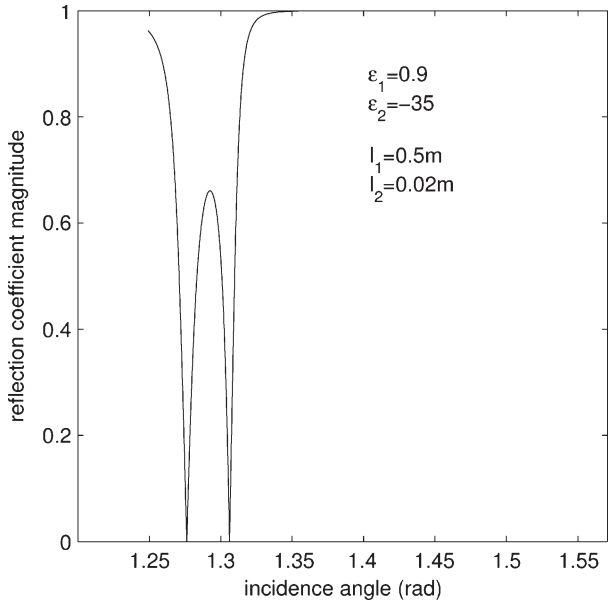

Fig. 13. Magnitude of the reflection coefficient versus the incidence angle in a three-layer structure for the boundary layer width $l_2 = 0.5$ m; the two corresponding resonant angles are $\theta = 1.277$ and $\theta = 1.306$.

the interval (1.533614, $\pi/2$). There are two resonant boundary layer widths for this case, both comparable in size to the plasma width l_2, particularly the smaller one. Comparing Figs. 11 and 12, one can see that there are two resonant boundary layer widths in both cases, but in Fig. 12, they are much smaller and much closer together. Absolute signal transmission occurs at the resonant boundary layer width. However, if a boundary layer width is chosen between those resonant values, one would expect a signal reflection of at most 27% for $\theta = 1.278$ and 51% for $\theta = 1.55$.

Consider once more Fig. 9. The minimum of this curve is at about $l_1 = 0.39$, which corresponds to a unique resonant incidence angle $\theta = 1.2910$ as shown in Fig. 8. For any resonant boundary layer width $l_1 > 1.079$, there is a unique resonant incidence angle. However, if we fix $l_1 \in (0.39, 1.079)$, then we will find two corresponding resonance incidence angles. Similarly, from Fig. 10, for any fixed resonant boundary layer width, there will be only one corresponding resonant incidence angle. In order for the boundary layer and the plasma to be comparable in size, we can choose $l_1 \in [0.0661, 0.08373]$. Observe in Fig. 10 that $\theta = 1.5078$ for $l_1 = 0.0661$ and $\theta = 1.533614$ for $l_1 = 0.08373$. Those ideas are shown in Fig. 13 for $l_1 = 0.5$ m and in Fig. 14 for $l_1 = 0.07$ m. In Fig. 13, the corresponding resonant incidence angles are $\theta = 1.276$ and $\theta = 1.306$. For those angles, absolute transparency will be achieved. Choosing an incidence angle between those two resonant angles, one can expect some transmission. In this case, the maximum reflection is about 66%. However, as we mentioned earlier, in this case, $l_1 \gg l_2$. On the other hand, in Fig. 14, l_1 is comparable with l_2, the unique corresponding resonant incidence angle is $\theta = 1.55$, and the bandwidth is quite large.

In summary, a three-layer structure permits one to choose a variety of resonant incidence angles and corresponding resonant boundary layer widths. By choosing an incidence angle closer to $\pi/2$, we can find a unique boundary layer width,

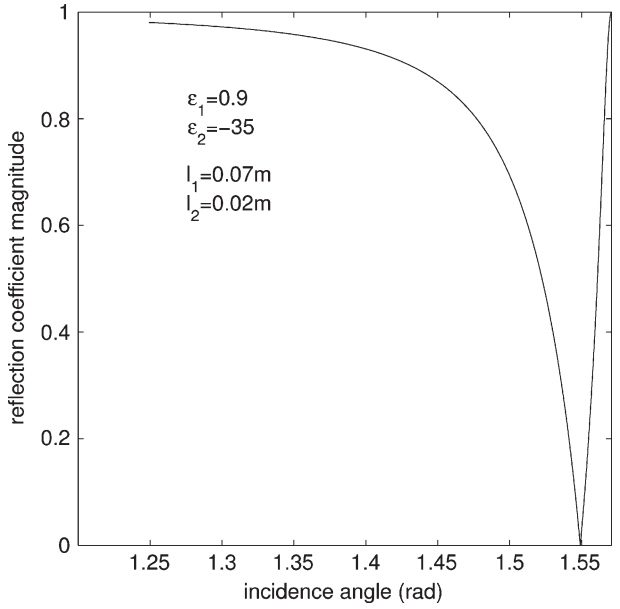

Fig. 14. Magnitude of the reflection coefficient versus the incidence angle in a three-layer structure for the boundary layer width $l_2 = 0.07$ m; the corresponding resonant angle is $\theta = 1.55$.

such that resonant transmission will be achieved. Moreover, the resonant boundary width is comparable in size with the plasma width, and the bandwidth could be adequate to ensure partial transmission in the neighborhood of the resonant incidence angle.

VI. Discussion

In this paper, we studied resonant transmission of electromagnetic waves through a three-layer structure, consisting of dense plasma ($\omega_{\rm pe} \gg \omega$) and two boundary layers of rarefied plasma on each side ($\omega_{\rm pe} < \omega$) shown in Fig. 6. For the dense plasma, we chose $\omega_{\rm pe}/\omega = 6$, which corresponds to the plasma permittivity $\epsilon_2 = -35$. For the plasma width, we chose $l_2 = 0.02$ m. Those parameters represent conditions that are relevant during hypersonic flight [8]. For the rarefied plasma, we chose the permittivity $\epsilon_1 = 0.9$, which corresponds to about $\omega_{\rm pe}/\omega = 0.3$. Under those conditions, the electromagnetic wave becomes evanescent in all three layers.

We have used an impedance method, which is convenient for studying multilayer structures and can easily be extended to study a large number of layers numerically. The impedance method enabled us to obtain analytical results for electromagnetic-wave transmission in a simple and transparent way and to gain a better understanding of that process. Our study clearly shows that in a two-layer structure, consisting of dense and rarefied plasma, transmission is induced by the resonance between the incident and the surface wave. For a two-layer structure, not every incidence angle will result in resonant conditions if the boundary layer permittivity is fixed. Studying the relationship between the resonant permittivity $0 < \epsilon_1 < 1$ and the resonant incidence angle θ, we found that ϵ_1 is increasing if θ is increasing and that ϵ_1 is close to one if θ is close to $\pi/2$. At the same time, as θ is increasing, the width of the boundary layer l_1 is decreasing. For a fixed ϵ_1, there is a unique pair (θ, l_1) which produces a surface-wave resonance, resulting in a 100% transmission of the electromagnetic wave. For example, for the parameters chosen earlier, we found that resonant transmission occurs only if the incident angle is $\theta = 1.2910$ and the width of the boundary is $l_1 = 0.78$ m. The resonant bandwidth is very narrow in this case. In order to reduce the width of the boundary layer, one needs to increase θ, which will result in an increase in ϵ_1.

By using the impedance method, we studied a symmetric three-layer structure and found the equation for the transparency condition. Unlike for two-layer structures, this equation permits multiple solutions for a surface-wave resonance. Those multiple solutions are related to the multiplicity of the resonant eigenmodes induced by coupling between the surface waves on each side of the dense-plasma layer. Studying the relationship between the resonant incidence angle and the resonant boundary layer width for the aforementioned parameters, we found three classes of incidence angles. With a high degree of accuracy, in the first class, $\theta \in (1.2761554, 1.27885]$. In the second class, $\theta \in [1.27885, 1.3087]$ as well as $\theta = 1.2761554$ and $\theta = 1.533614$. In the third class, $\theta \in (1.533614, \pi/2)$. For each θ in the second class, there is a unique resonant boundary layer width which results in a 100% transmission of the electromagnetic wave. For each θ in the first and third classes, there are two resonant boundary layer widths. For the first class of angles, the resonant boundary layer widths are much larger than the plasma width, while for the third class, the boundary layer width is comparable to the plasma width. Similarly, we can find three classes for the resonant boundary layer width (measured in meters): $l_1 > 1.079$, $l_1 \in [0.39, 1.079]$, and $l_1 \in [0.06661, 0.08373]$. Note that the boundary layer widths in the first and second classes are much larger than the width of the plasma layer. For each l_1 in the second class, there are two resonant incidence angles. For those angles, absolute transparency can be achieved. Choosing an incidence angle between the resonant incidence angles, one can achieve partial transparency. For each l_1 in the first and third classes, there is a unique resonant incidence angle. In particular, choosing l_1 in the third class, such that it is comparable to the plasma width, we showed that the corresponding incidence angle is close to $\pi/2$ and the bandwidth is quite large.

In summary, for a three-layer structure, one can observe total transmission of an electromagnetic wave by inducing a surface-wave resonance. This can be achieved by choosing an adequate incidence angle and a corresponding boundary layer width. For an incidence angle close to $\pi/2$, the boundary layer width is comparable in size to the width of the plasma layer. In this case, the bandwidth may be sufficiently large to achieve at least partial transmission.

Our study shows that, in general, surface-wave resonance can be used to amplify evanescent waves, in order to achieve transparency of dense plasmas in special configurations such as in the particular two- and three-layer structures we have discussed. There are certain limitations of our model that would have to be addressed in the future to clarify its applicability to the problem of communications through dense plasmas [9]–[13]. First, we assumed that the plasma layers are homogeneous and that there is a sharp interface between them. It

remains to be investigated how the surface-wave dispersion relations and resonant conditions such as given by (42) will change when a smooth transition occurs between the layers of different plasma density. Second, we neglected the role of electron–atom collisions and electron temperature. In general, the dissipation caused by electron–atom collisions and by electron thermal motion will adversely affect the resonant transmission. The effects of dissipation are particularly detrimental for the narrow resonance situation (equivalent to the system of high quality factors). On the other hand, electron thermal motion effects lead to the appearance of new resonant modes and additional transparency regimes [15]. Lastly, 2-D effects have to be considered [9]. All those questions go beyond the scope of this paper and are left for future studies.

REFERENCES

[1] H. Raether, *Surface Plasmons on Smooth and Rough Surfaces and on Gratings*. Berlin, Germany: Springer-Verlag, 1988.

[2] W. L. Barnes, A. Dereux, and T. W. Ebbesen, "Surface plasmon subwavelength optics," *Nature*, vol. 424, no. 6950, pp. 824–830, Aug. 2003.

[3] J. B. Pendry and D. R. Smith, "The quest for the superlens," *Sci. Amer.*, vol. 295, no. 1, pp. 60–67, Jul. 2006.

[4] A. Alù and N. Engheta, "Achieving transparency with plasmonic and metamaterial coating," *Phys. Rev. E, Stat. Phys. Plasmas Fluids Relat. Interdiscip. Top.*, vol. 72, no. 1, p. 016 623, Jul. 2005.

[5] J. B. Pendry, "Photonics: Metamaterials in the sunshine," *Nat. Mater.*, vol. 5, no. 8, pp. 599–600, Aug. 2006.

[6] N. Sternberg and V. Godyak, "Approximation of the bounded plasma problem by the plasma and the sheath models," *Phys. D*, vol. 97, no. 4, pp. 498–508, Oct. 1996.

[7] N. Sternberg and V. Godyak, "Asymptotic matching and the sheath edge," *IEEE Trans. Plasma Sci.*, vol. 31, no. 4, pp. 665–677, Aug. 2003.

[8] E. Josyula and W. Bailey, "Governing equations for weakly ionized plasma flowfields of aerospace vehicles," *J. Spacecr. Rockets*, vol. 60, no. 6, pp. 845–857, Jun. 2003.

[9] M. White and S. Sherer, "High-order simulation of communication through a weakly ionized plasma for reentry vehicles," in *Proc. 44th AIAA Aerosp. Sci. Meeting Exhib.*, Reno, NV, Jan. 9–12, 2006.

[10] R. Rawhauser, *Propagation Factors in Space Communications*, W. T. Blackband, Ed. Maidenhead, U.K.: Technivision, 1967, p. 327.

[11] R. Betchov and E. A. Fuhs, *Electromagnetic Aspects of Hypersonic Flight*, W. Rothman, H. K. Moore, and R. Papa, Eds. Baltimore, MD: Spartan, 1964.

[12] M. P. Bachynski, *Propagation Factors in Space Communications*, W. T. Blackband, Ed. Maidenhead, U.K.: Technivision, 1967, p. 287.

[13] S. V. Nazarenko, A. C. Newell, and V. E. Zakharov, "Communication through plasma sheath via Raman (three-wave) scattering process," *Phys. Plasmas*, vol. 1, no. 9, pp. 2827–2834, Sep. 1994.

[14] A. Alù and N. Engheta, "Pairing an ϵ-negative slab with a μ-negative slab: Resonance, tunneling and transparency," *IEEE Trans. Antennas Propag.*, vol. 51, no. 10, pp. 2558–2571, Oct. 2003.

[15] E. Fourkal, I. Velchev, C.-M. Ma, and A. Smolyakov, "Evanescent wave interference and total transparency of warm high-density plasma slab," *Phys. Plasmas*, vol. 13, no. 9, pp. 092 113-1–092 113-9, Sep. 2006.

[16] R. Dragila, B. Lutherdavies, and S. Vukovic, "High transparency of classically opaque metallic films," *Phys. Rev. Lett.*, vol. 55, no. 10, pp. 1117–1120, Sep. 1985.

Natalia Sternberg was born in Czernowitz, Ukraine, on April 7, 1954. She received the M.S. degree in mathematics from the University of Cologne, Cologne, Germany, in 1979, and the M.S. and Ph.D. degrees in applied mathematics from Brown University, Providence, RI, in 1982 and 1985, respectively.

From 1985 to 1987, she was a Visiting Assistant Professor with Northeastern University, Boston, MA, and Brown University. Since 1987, she has been with Clark University, Worcester, MA, where she is currently a Professor of mathematics and computer science. Her research interest includes developing analytical and numerical methods to study the dynamical properties of solutions of differential equations that occur in physical and biological models. She is currently working on mathematical models in plasma science.

Andrei I. Smolyakov was born in Ukraine in 1959. He received the M.Sc. degree in plasma physics and chemistry in 1983 and the Candidate of Physical and Mathematical Sciences degree in 1986, both from the Moscow Institute of Physics and Technology, Moscow, Russia.

From 1986 to 1995, he was with the Theoretical Division, Department of Plasma Physics, Kurchatov Institute of Atomic Energy (currently Institute for Nuclear Fusion, Russian Research Center "Kurchatov Institute"), Moscow. During this time, he also taught at the Department of General Physics, Moscow Institute of Physics and Technology. Since 1995, he has been with the Department of Physics and Engineering Physics, University of Saskatchewan, Saskatoon, SK, Canada, where he is currently a Professor. His research interests include nonlinear plasma theory, MHD and transport phenomena in magnetically confined plasmas, physics of low-temperature gas discharges, and plasmonics.

Prof. Smolyakov is a Fellow of the American Physical Society.